

Investigation of polymer electrolytes based on agar and ionic liquids

R. Leones¹, F. Sentanin², L. C. Rodrigues¹, I. M. Marrucho³, J. M. S. S. Esperança³, A. Pawlicka², M. M. Silva^{1*}

¹Centro de Química, Universidade do Minho, Gualtar, 4710-057 Braga, Portugal

²Instituto de Química de São Carlos, Universidade de São Paulo, CxP 780, 13560-970 São Carlos, SP, Brazil

³Instituto de Tecnologia Química e Biológica, Universidade Nova de Lisboa, www.itqb.unl.pt, 2780-157 Oeiras, Portugal

Received 8 May 2012; accepted in revised form 28 July 2012

Abstract. The possibility to use natural polymer as ionic conducting matrix was investigated in this study. Samples of agar-based electrolytes with different ionic liquids were prepared and characterized by physical and chemical analyses. The ionic liquids used in this work were 1-ethyl-3-methylimidazolium ethylsulfate, [C₂mim][C₂SO₄], 1-ethyl-3-methylimidazolium acetate, [C₂mim][OAc] and trimethyl-ethanolammonium acetate, [Ch][OAc].

Samples of solvent-free electrolytes were prepared and characterized by ionic conductivity measurements, thermal analysis, electrochemical stability, X-ray diffraction, scanning electron microscopy and Fourier Transform infrared spectroscopy. Electrolyte samples are thermally stable up to approximately 190°C. All the materials synthesized are semicrystalline. The electrochemical stability domain of all samples is about 2.0 V *versus* Li/Li⁺. The preliminary studies carried out with electrochromic devices (ECDs) incorporating optimized compositions have confirmed that these materials may perform as satisfactory multifunctional component layers in the field of ‘smart windows’, as well as ECD-based devices.

Keywords: biodegradable polymers, smart polymer, thermal properties, Agar matrix

1. Introduction

Polymer electrolytes (PEs) are ionically conducting materials that may be used in the fabrication of solid-state electrochemical devices, particularly rechargeable batteries, electrochromic displays, capacitors and sensors [1, 2]. During the last decades different systems have been extensively studied and most of them were based on poly(ethylene oxide) [2]. More recently new types of electrolytes based on natural polymers (like cellulose derivatives, chitosan, starch or natural rubber) have been proposed due to their biodegradability, low production cost, good physical and chemical properties and good performance as SPEs (solvent-free polymer electrolytes) [3–5]. Among these there is agar, which is an heterogeneous mixture of agarose and agarose

[6]. Recently, natural macromolecules are the goal of the new materials research tendencies due to the increasing alerts concerning the contribution of synthetic polymers to the environmental destruction [7, 8]. The main argument for the use of bio-macromolecules is their extraction from renewable sources, as fast growing plants, animals and crustacean or also by bacterial synthesis [9, 10] and consequently their biodegradation properties.

In spite of SPEs potential, their application in commercial devices has been delayed because of their tendency to crystallize, substantially lower ionic conductivity than non-aqueous liquid electrolytes and a tendency to salt exudation at high salt concentration. However, as liquid electrolytes pose significant safety and environmental concerns, in recent

*Corresponding author, e-mail: nini@quimica.uminho.pt

years considerable efforts have been devoted to increase the ionic conductivity and improve the mechanical properties of SPEs [1, 2].

In order to do so, many research groups turned their attention to room temperature ionic liquids (RTILs) [11]. The introduction of ionic liquids (ILs) into macromolecules structure has been presented as a very interesting way to obtain good ionic conductivity without liquid components [12–14]. These polymer electrolytes based on ILs have been developed for battery electrolyte and for other solid electrolyte applications [15, 16]. It was successfully demonstrated that the electrochemical stability and ionic conductivity of SPEs are enhanced by the addition of ILs. Also, their addition ensures safety, owing to some intrinsic properties of ILs such as their almost zero volatility [17], zero flammability [18] and high thermal stability [19].

This paper describes the preparation and characterization of agar-based polymer electrolytes with ionic liquids as guest salts. Looking for good conductivity results combined with transparency, flexibility, good adhesion, good mechanical and electrochemical properties, electrolytes were characterized by conductivity measurements, thermal analysis (DSC and TGA), cyclic voltammetry, X-ray diffraction (XRD) and scanning electron microscopy (SEM). These materials were also tested as ionic conductors in electrochromic devices with the following configuration: glass/ITO/WO₃/PolymerElectrolyte/CeO₂-TiO₂/ITO/glass.

2. Experimental

2.1 Materials

Ionic liquids. The ionic liquids used in this work were 1-ethyl-3-methylimidazolium ethylsulfate (IL-0033-HP/342573-75-5), [C₂mim][C₂SO₄], 1-ethyl-3-methylimidazolium acetate (IL-0189-TG/143314-17-4), [C₂mim][OAc] and trimethyl-ethanolammonium acetate, [Ch][OAc]. [C₂mim][C₂SO₄] and [C₂mim][OAc] were supplied by Iolitec (Heilbronn, Germany) with a stated purity of 99 and 95%, respectively. [Ch][OAc] was supplied by Solchemar with a purity of 95%. To reduce the water and other volatile substances contents, vacuum (10 Pa) and moderate temperature (ca. 47°C) were always applied to all samples of ionic liquids for several days prior to their use. After degassing, the purity was checked by ¹H NMR. The ¹H spectra confirmed purity levels

higher than 99% for [C₂mim][C₂SO₄] and 98% for [C₂mim][OAc] and [Ch][OAc]. The final water mass fraction was measured by Karl Fischer coulometric titration (Metrohm 831 KF Coulometer). The dried samples contained less than 500 ppm of water for all ionic liquids.

2.2. Sample preparation

Samples were prepared according to a procedure optimized by E. Raphael *et al.* [6]. In a glass flask, 0.5 g of agar (W201201, Aldrich, Madrid, Spain) was dispersed in 30 mL of Milli-Q water and heated under magnetic stirring for a few minutes up to 100°C for complete dissolution. Next, 0.5 g of ILs, 0.5 g of glycerol (RM1027-1L, Himedia, Mumbai, India, 99.5%) as plasticizer, 0.5 g of formaldehyde as crosslinking agent (131328, Panreac, Barcelona, Spain, 37–38% wt/wt), were added to this solution under stirring. This solution was then poured on Petri plates, let to dry up for 8–10 days at ambient temperature, to form transparent membranes. The film was transferred to an oven at 60°C, for final drying, and the sample was aged for a period of 1 week resulting in the homogeneous and transparent membranes with thickness of 150 μm as shown in Figure 1.



Figure 1. Physical appearance of a sample, incorporating the [C₂mim][OAc]

2.3. Measurements

2.3.1. Ionic conductivity

The total ionic conductivity of the samples was determined by locating an electrolyte disk between two 10 mm diameter ion-blocking gold electrodes (Goodfellow, >99.95%) to form a symmetrical cell.

The electrode/polymer electrolyte/electrode assembly was secured in a suitable constant volume support and installed in a Büchi TO51 tube oven with a type K thermocouple placed close to the electrolyte disk to measure the sample temperature. Bulk conductivities of the electrolyte samples were obtained during heating cycles using the complex plane impedance technique (Autolab PGSTAT-12 (Eco Chemie)) between 25 and 100°C and at approximately 7°C intervals.

2.3.2. Thermal analysis

The DSC measurements were performed under a flowing nitrogen atmosphere at 30 mL·min⁻¹ in the temperature range of -110 to 200°C and at a heating rate of 20°C·min⁻¹ using a TA Instruments DSC-Q20 apparatus. The first run was up to 100°C to remove adsorbed water and the second and third runs were performed up to 200°C.

Samples for thermogravimetric studies were prepared in a similar manner, transferred to open crucibles and analyzed using a Rheometric Scientific TG1000 thermobalance operating under flowing argon, between 30 and 700°C and at a heating rate of 10°C·min⁻¹.

2.3.3. Electrochemical stability

The evaluation of the electrochemical stability window of electrolyte compositions was carried out under an argon atmosphere using a two-electrode cell configuration. The preparation of a 25 µm diameter gold microelectrode surface, by polishing it with a moist cloth and 0.05 µm alumina powder (Buehler), was completed outside the drybox. The cell was assembled by locating a clean lithium disk counter electrode (cut from Aldrich, 99.9%, 19 mm diameter, 0.75 mm thick) on a stainless steel current collector and centering a sample of electrolyte on the electrode surface. A small volume (2 µL) of THF was placed on the microelectrode surface. The microelectrode was then located on the electrolyte surface and supported firmly by means of a clamp. The use of THF to soften the electrolyte was necessary to achieve a reproducible microelectrode/electrolyte interfacial contact. An Autolab PGSTAT-12 (Eco Chemie) was used to record voltammograms at scan rate of 30 mV/s. Measurements were performed at room temperature, within a Faraday cage.

2.3.4. X-ray diffraction

The structure of the film was examined on silicon wafer by X-ray Rigaku Ultima 4 diffractometer, power of 50 kV/50 mA and CuKα irradiation, speed of 2 °/min, in an angle range (2θ) of 5 to 60°, at room temperature.

2.3.5. SEM

SEM micrographies were obtained with LEO model 440.

2.3.6. FTIR

Infrared spectra were measured by using an ATR-FTIR BOMEM MB 102 spectrophotometer. The films were placed in the holder directly in the IR laser beam. Spectra were recorded in scanning range from 650 to 4000 cm⁻¹ at a resolution of 4 cm⁻¹ and 16 scans.

2.3.7. Electrochromic cell assembly

Electrochromic devices with the configurations glass/ITO/WO₃/electrolyte/CeO₂-TiO₂/ITO/glass were obtained by assembling the 2 pieces of coated glasses. Electrolytes in the form of hydrated membranes were deposited on glass/ITO/WO₃ coatings and 1 cm free space was left for the electrical contact. Then the other coated substrate was pressed onto the membrane in such a way that the two coatings faced each other inside the assembled window. A 1 cm wide Cu-conducting tape (3M) was glued to the free edge of each substrate for electrical connection. The mounted cells were finally sealed with a protective tape (3M).

The electrochemical measurements were performed with Autolab 302N with FRA 2 module.

3. Results and discussion

3.1. FTIR analysis

The infrared spectra of the pure agar membrane and of the membranes containing agar and ionic liquids are shown in Figure 2. In this figure it is observed a significant change in the FTIR spectra with the addition of ionic liquids. The broadband at 3416 cm⁻¹, attributed to the stretching of OH hydroxyl groups of agar that participate in hydrogen bond formation in inter- and intramolecular bonds or in hydrogen inter and intramolecular bond formation, shifts to shorter wavelengths numbers with the addition of

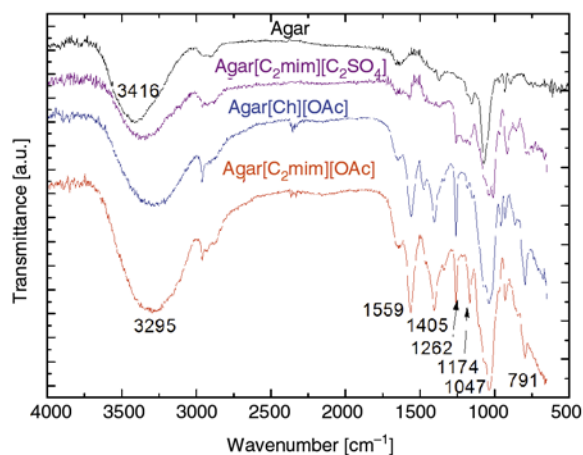


Figure 2. FTIR spectra of agar and agar-based membranes

ILs [20, 21]. The bands at 2934 and 2887 cm^{-1} refer to the CH asymmetrical stretching, which increase in intensity due to its presence in both glycerol and in the ILs [22, 23]. The band at 2360 cm^{-1} is due to the CO_2 from air and at 1653 cm^{-1} is due to adsorbed water. Samples with ILs present a new band at 1559 cm^{-1} , probably due to C=C imidazolium ring [24] assigned to be at 1562 cm^{-1} [23]. The shift of this band is also an indication of interaction between polysaccharide and IL. The band at 1405 cm^{-1} is assigned to CH bending. The sharp bands at 1262 cm^{-1} in the FTIR spectra of the samples with [Ch][OAc] and [C₂mim][OAc] are probably due to C–C stretching in the sample Agar[C₂mim][C₂SO₄] can be due to C–O–SO₃ asymmetric stretching. The bands at 1174 cm^{-1} can be assigned to C–O–C from agar as in the case of cellulose dissolved in the 1-butyl-3-methylimidazolium chloride [23] and at 1168 cm^{-1} to ring in-plane asymmetric stretching, C–C and (N)CH₂ stretching [25]. The stretching of the COH alcohol bond shifts from 1087 to 1038 cm^{-1} , which is probably due to the hydrogen bond formation between glycerol and macromolecule. Other bands from 920 to 960 cm^{-1} , depending on the sample, can be assigned to C–O–SO₃ or C–C stretching from polymer ring [26] and at 780; 790 cm^{-1} to IL ring HCCH symmetric bending [22] or 3,6-anhydro- β -galactose skeletal bending [26].

3.2. Thermal behaviour of electrolytes

The onset of thermal decomposition was estimated through thermogravimetric analysis (Figure 3). All samples show a weight loss of 5% for the pure agar membrane, Agar[C₂mim][C₂SO₄], and Agar[C₂mim][OAc] and 18% for the sample Agar[Ch][OAc] in

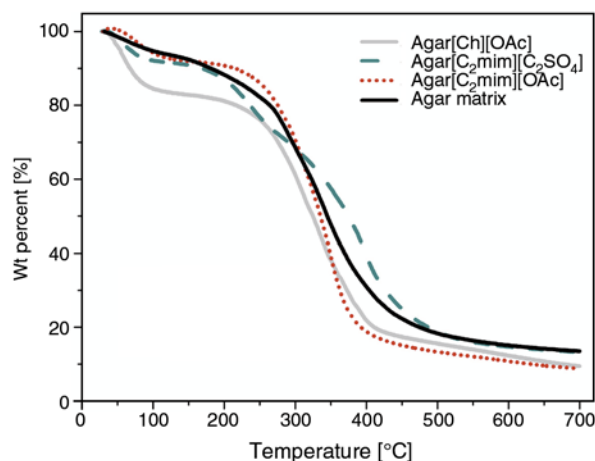


Figure 3. TGA results for membranes based agar and ionic liquids

between room temperature and about 100°C, which can be explained as a water loss in the sample. The moisture content (as observed in FTIR spectra and also DSC first run) in the Agar[Ch][OAc] is higher when compared to agar and Agar[C₂mim] samples probably due to the hydrophilic properties of the choline ion. In the region of 220–400°C, the film of agar matrix showed a very accentuated mass loss of 65%, which marks the decomposition of the sample, and slowly continues as the temperature is increased up to 700°C. The remaining residue was 15% in mass of the starting material. In the case of the samples with ILs, the loss mass behavior as a function of temperature is different. The degradation process occurs in two stages for the agar based electrolytes with [C₂mim][C₂SO₄], assuming that the negligible initial mass loss observed (<5%) is exclusively associated with the release of solvents, such as water adsorbed or coordinated. For these samples the first stage starts at 200°C for a weight percent of 90% and the second starts at 300°C for a weight percent of 68%. These stages are due to the agaropectin and agarose presence in the samples and the different interactions with ILs. The onset temperature of thermal decomposition was estimated by thermogravimetric analysis using extrapolation of the baseline and tangent of the curve of thermal events to identify the initiation of sample weight loss. The degradation process occurs in one stage for the agar based electrolytes with Agar[C₂mim][OAc] and Agar[Ch][OAc], assuming that the negligible initial mass loss observed (<5% for sample Agar[C₂mim][OAc] and <20% for Agar[Ch][OAc]) is exclusively associated with the release of solvents,

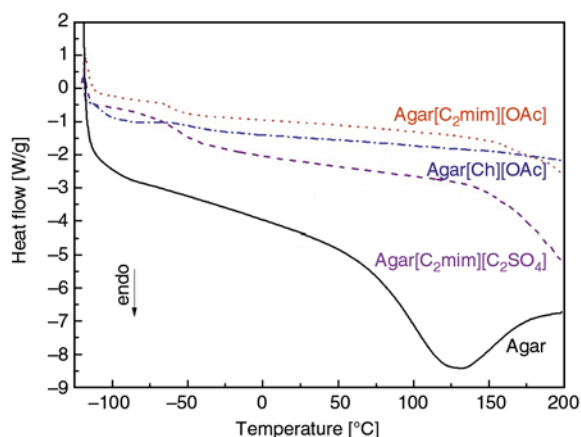


Figure 4. DSC curves obtained for membranes of Agar[C₂mim][C₂SO₄] (— — —), Agar[C₂mim][OAc] (· · ·) and Agar[Ch][OAc] (- · - · -)

such as water adsorbed or coordinated. The polymer electrolyte Agar[Ch][OAc] loses more solvents probably because the [Ch][OAc] IL used had more water. The second stage of the samples degradation for a mass loss of 80% starts at 200°C and ends at 550°C and slowly continues at 700°C. The remaining residue was 10% for the samples Agar[C₂mim][OAc] and Agar[Ch][OAc].

The DSC results obtained for the materials are illustrated in Figure 4 and in all cases a very accentuated change of the baseline is observed at -58, -60 and -44°C for the samples Agar[C₂mim][C₂SO₄], Agar[C₂mim][OAc] and Agar[Ch][OAc], respectively. It was already reported that glass transition in agar samples can be found or observed in the range of temperature between 60 and 130°C depending on the molecular mass and moisture content [27, 28]. However, no linebase changes were observed in the agar matrix used for this study. Therefore, the change of baseline in Figure 4 is probably due to the T_g of glycerol-rich domains [25] or also to glycerol-water [29] or glycerol-agar associations. This last supposition/possibility can be supported by other studies on natural macromolecules gel membranes with glycerol as plasticizer [5]. Above 150°C two samples, Agar[C₂mim][C₂SO₄] and Agar[C₂mim][OAc], exhibit a start of an endothermic peak, attributed to the start of the degradation of the sample, as observed by TGA measurements. No endothermic peak up to 200°C is observed for the sample Agar[Ch][OAc]. The obtained results confirm that all the polymer electrolytes produced have predominantly amorphous nature.

3.3. Structure and morphology

Figure 5 shows the typical X-ray diffraction patterns obtained for the sample Agar[C₂mim][C₂SO₄] measured at room temperature. The diffractogram of agar matrix (not shown here) revealed an ordered structure due to the presence of a very accentuated peak at 18.6° 2 θ and a slight shoulder at 14.3° 2 θ , similarly to the results of 19.9 and 13.83°, respectively, reported for pristine agar films [30]. The deconvolution of the diffraction profile (Figure 5) in different Gaussian lines reveals very broad components on the fully disordered part of the sample and the three narrower bands are attributed to the ordered regions. From the deconvoluted plot, the degree of crystallinity of this sample is found to be about 25%. Moreover, through the SEM pictures one can observe the homogeneity without any phase separation and good surface uniformity of agar-based electrolyte with ionic liquid samples (Figure 6). Agar-ILs-based SPE samples were translu-

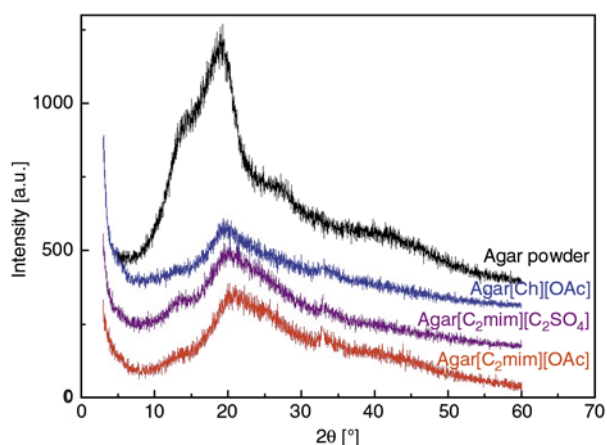


Figure 5. X-ray diffractogram for agar matrix and agar-based membranes on glass XDR support

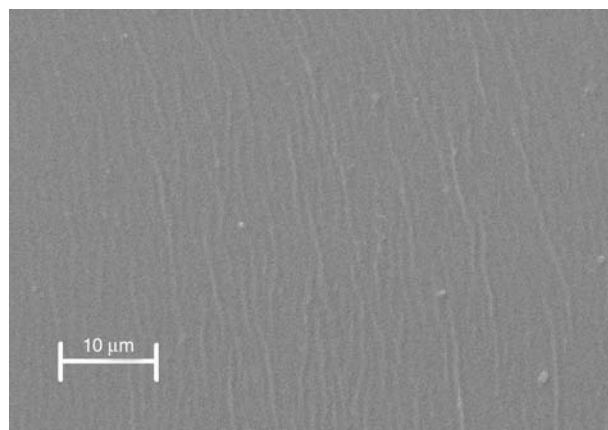


Figure 6. SEM picture of the sample, incorporating the [C₂mim][C₂SO₄]

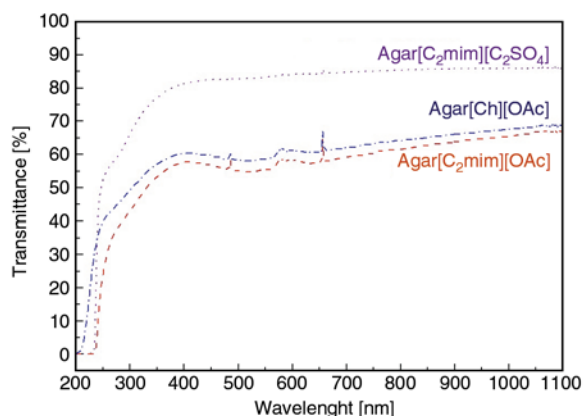


Figure 7. Optical transmittance measurement for membranes of Agar[C₂mim][C₂SO₄] (---), Agar[C₂mim][OAc] (···) and Agar[Ch][OAc] (-·-·-)

cent (Figure 1) and showed very good adhesion properties to glass and steel.

Figure 7 shows the optical transmittance of a 0.52, 0.12 and 0.46 mm thick layer of the Agar[C₂mim][C₂SO₄], Agar[C₂mim][OAc] and Agar[Ch][OAc] electrolytes as well as almost zero transmission intensity below 230 nm, which starts to increase until reaching 81, 57 and 60% at 400 nm, respectively. For the 400 to 1100 nm wavelength interval the transmission is practically constant increasing only few percent. From the obtained results it is possible to observe that ILs with acetate ion promote a decrease of the transparency similar to a previous study [31, 32].

3.4. Ionic conductivity of electrolytes

The ionic conductivities of various polymer electrolytes over the temperature range from 25 to 105°C and as a function of different ionic liquids are illustrated in Figure 8. From this figure we can observe that all samples exhibit a linear variation of log conductivity with reciprocal temperature, which is typical of polymer electrolytes where hopping mechanism of ionic charge species is predominant. From this figure it is also possible to observe that the addition of any ILs studied, produces an increase of ionic conductivity values, when compared to the matrix. The highest room temperature ($T = 30^\circ\text{C}$) conductivity of the electrolyte system is $2.35 \cdot 10^{-5} \text{ S}\cdot\text{cm}^{-1}$, registered for the agar based on 1-ethyl-3-methylimidazolium acetate composition. At 100°C , this electrolyte exhibits a conductivity of about $1.58 \cdot 10^{-3} \text{ S}\cdot\text{cm}^{-1}$. The small differences in the conductivity values as a function of temperature of

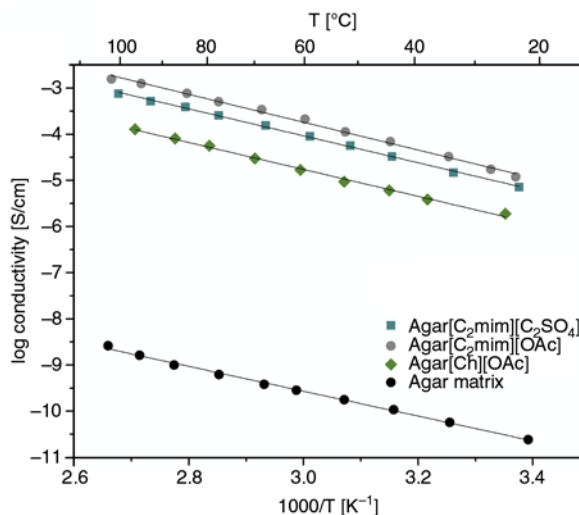


Figure 8. Variation of ionic conductivity with $1/T$ for selected electrolyte

the samples with ILs may be due to the type of ILs, its dielectric constant, viscosity, interaction with the host polymer and molecular weight [33]. The temperature dependence of the ionic conductivity values shows an Arrhenius behavior, where the ionic transport is promoted by the hopping of ionic species. In this, the ILs probably promotes a better separation of polymeric chains and, consequently, its more pronounced movements.

The fitted value of the E_a for the electrolyte based on 1-ethyl-3-methylimidazolium acetate is $24.27 \text{ K}\cdot\text{J}\cdot\text{mol}^{-1}$. This is smaller than those reported by Raphael *et al.* [6] for agar-acetic acid-based electrolytes or other natural macromolecules [31, 32, 34]. The E_a values decrease with the addition of ILs and this is in agreement with the fact that the amount of ions in polymer electrolyte increases, and the energy barrier to the ion transport decreases, leading to a decrease in the activation energy.

3.5. Electrochemical stability

Cyclic voltammetry was employed to evaluate the chemical and electrochemical stability of the solid polymer electrolytes. In the cyclic voltammetric analysis the sweep potential was firstly scanned in the positively going direction and then the reversed direction. The addition of ionic liquid doesn't deplete the electrochemical stability of the electrolytes. A very low current flow was observed up to the anodic breakdown voltage, thus supporting the high purity of the RTIL-based polymer electrolytes.

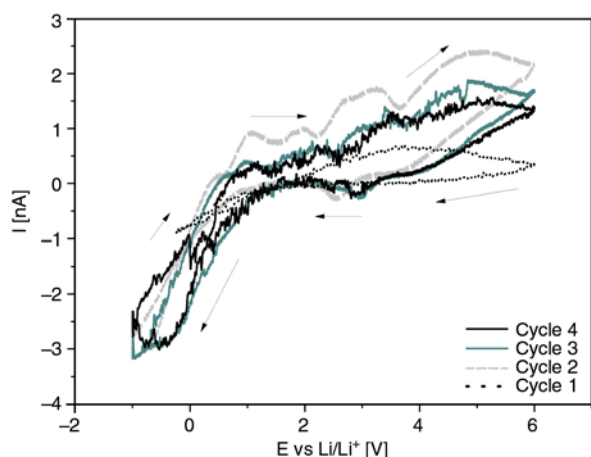


Figure 9. Voltammogram of the Agar[C₂mim][C₂SO₄] sample at a 25 μm diameter gold microelectrode versus Li/Li⁺. Initial sweep direction is anodic and different sweep rate.

The electrochemical stabilities of the polymer electrolytes based on ILs (Figure 9) were determined by microelectrode cyclic voltammetry over the potential ranging from -2.0 to 6.0 V at scan rate $30 \text{ mV}\cdot\text{s}^{-1}$ and at ambient temperature. The anodic current onset may be associated with the decomposition of the polymer electrolyte. The voltammetric stability of the electrolytes containing ILs was checked by the repetitive potential sweep at a scan rate of $30 \text{ mV}\cdot\text{s}^{-1}$. The results are shown in Figure 9. The peak currents decrease with the increase of the scan numbers, which may be due to the detach of the samples from the electrode surface.

It is noted that a small reduction peak around 1.5 – 2.0 V appeared for the electrolytes films based on [C₂mim][C₂SO₄] (Figure 9). Previously, the peak in this region had been ascribed to the reduction of low level of water present in IL or oxygen impurities. These measurements are made in glove box and probably oxygen impurities are not present. Similar behavior has been observed for other systems based on PEO, lithium salt and IL [35].

As can be seen, all the electrolytes show good stability of 2.0 V windows versus Li/Li⁺. They display a wide electrochemical window (-2.0 to $+2.0$ V) over which the polymer electrolytes based on ILs can be used safely without decomposition. A large electrochemical window is a valuable property for the fabrication of stable and durable electrochemical devices.

3.6. Electrochromic device

A preliminary evaluation of the performance of the agar based materials as electrolytes in all solid-state ECDs was carried out using the five layer-sandwich configuration.

Typical cyclic voltammograms of an ECD containing Agar[C₂mim][C₂SO₄] measured during the 10th, 50th, 100th, 150th and 200th chronoamperometric cycles are shown in Figure 10. One cathodic peak centered at -1.3 V is observed and is accompanied by the coloring of the device while the other, centered around -0.3 V, is anodic and is accompanied by the bleaching of the device. The feature of the voltammograms doesn't change during 200 cycles, however a small shift to more positive potentials is observed.

The charge density responses measured by chronoamperometry (-2 V/ $+1.8$ V; $15 \text{ s}/15 \text{ s}$) of ECD containing solid electrolyte based on agar and ILs for the cycle 10th, 50th, 100th, 150th and 200th are shown in Figure 11. From these measurements, it can be stated that the insertion (coloration) is fast. For instance, for the 10th cycle, the inserted charge at -2 V reaches $-0.76 \text{ mC}\cdot\text{cm}^{-2}$ in 15 s . The consecutive chronoamperometric cycling promotes a decrease of the inserted charge values reaching $-0.4 \text{ mC}\cdot\text{cm}^{-2}$ for the 200 cycles. The reverse potential, i.e., $+1.8$ V promotes an extraction and consequent bleaching of the device. This phenomenon occurs faster than coloring and after 2 s the ECD is already transparent. However, as can be observed from this experiment for the initial cycles extracted charge value is lower when compared with the inserted one, indicating

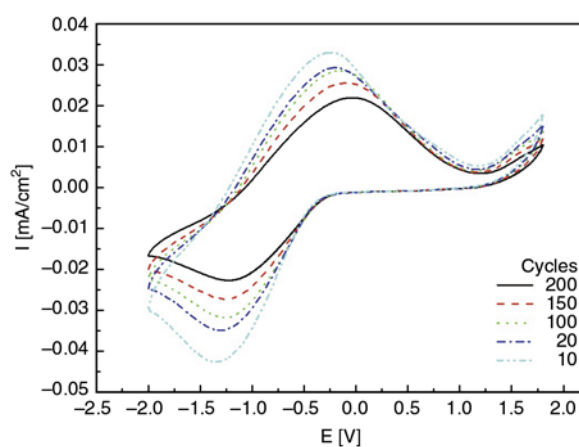


Figure 10. Cyclic voltammograms of electrochromic window with WO₃/Agar[C₂mim][C₂SO₄]/CeO₂-TiO₂ configuration

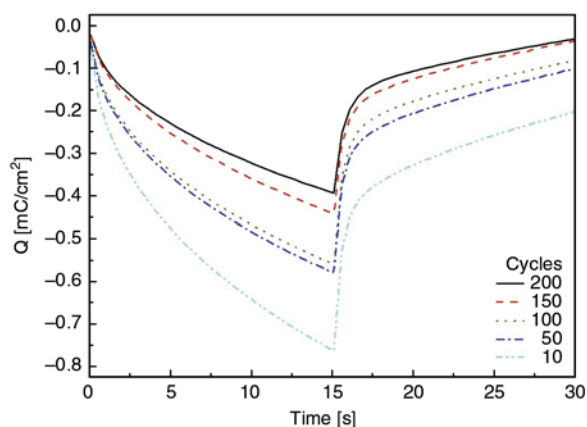


Figure 11. Charges densities for ECDs electrochromic window with $\text{WO}_3/\text{Agar}[\text{C}_2\text{mim}][\text{C}_2\text{SO}_4]/\text{CeO}_2\text{-TiO}_2$ configuration of 10th to 200th cycles

that some part of the charge remains in the electrochromic coating and is probably responsible for the not complete reversibility of the device. As a consequence a successive decrease of the inserted charge density as a function of number of cycles is observed.

The UV-vis transmission spectra of the electrochromic device in the range from 200 to 1100 nm for the 200th cycle are measured (not shown). A transmittance variation of 13% between the bleached (63% of transmittance) and colored states (50% of transmittance) occurs in the visible range of the spectra with a maximum at 550 nm. This result is comparable to the results obtained with electrochromic devices containing ormolytes-based electrolytes with potassium salt [36]. The promising tests performed in the present work based on ILs support the idea that these materials may find application in polymer science, like others [37].

4. Conclusions

Polymer electrolytes based on agar and containing ILs were prepared and characterized. The obtained results revealed that the ILs influence the ionic conductivity of electrolytes and the best values of $2.35 \cdot 10^{-5} \text{ S}\cdot\text{cm}^{-1}$ were registered for the agar based on 1-ethyl-3-methylimidazolium acetate composition at ambient temperature. At 100°C, this electrolyte exhibits a conductivity of about $1.58 \cdot 10^{-3} \text{ S}\cdot\text{cm}^{-1}$. These results show a Arrhenius behavior with an activation energy of $E_a = 24.27 \text{ kJ/mol}$.

In ECDs very specific conditions must be fulfilled by the electrolyte component. These include high

transparency to maximize chromatic contrast in the case of see-through displays, adequate room temperature conductivity to permit rapid color response, mechanical flexibility to form an appropriate electrode/electrolyte interface and low thermal expansion or component volatility so that the device may operate over a wide range of temperatures. The samples applied in small electrochromic devices evidenced the reversible insertion/extraction process during 200 chronoamperometric cycles. The inserted charge was $-0.40 \text{ mC}\cdot\text{cm}^{-2}$ during 15 s and the extraction occurred in 2 s.

The encouraging results of the thermal (DSC and TGA), electrochemical (ionic conductivity and CV), and structural (XRD) investigation of a novel series of agar – ILs membranes are sufficient to justify further studies. The preliminary tests performed in this study using prototype ECDs suggest that these materials may find application in ‘smart windows’ devices, as well as other electrochromic displays.

Acknowledgements

The authors are pleased to acknowledge the support provided by the University of Minho and the Fundação para a Ciencia e a Tecnologia for laboratory equipment and research staff grants (contracts project n^oF-COMP-01-0124-FEDER-022716 (ref^a FCT PEst-C/QUI/UI0686/2011) FEDER – COMPETE, FCT – Portugal, PEst-OE/EQB/LA0004/2011, PTDC/CTM-NAN/121274/2010 and SFRH/BD/38616/2007). The authors are indebted to FAPESP, CAPES and CNPq, for the financial support given to this research.

References

- [1] Armand M. B., Chabagno J. M., Duclot M. T.: Polymeric solid electrolytes. in ‘Proceeding of the Second International Meeting on Solid State Electrolytes, St. Andrews, Scotland’ 6.5.1. (1978).
- [2] Gray F. M.: Solid polymer electrolytes: Fundamentals and technological applications. VCH, New York (1991).
- [3] Pawlicka A., Danczuk M., Wieczorek W., Zygadlo-Monikowska E.: Influence of plasticizer type on the properties of polymer electrolytes based on chitosan. *Journal of Physical Chemistry A*, **112**, 8888–8895 (2008). DOI: [10.1021/jp801573h](https://doi.org/10.1021/jp801573h)
- [4] Avellaneda C. O., Vieira D. F., Al-Kahlout A., Leite E. R., Pawlicka A., Aegerter M. A.: Solid-state electrochromic devices with $\text{Nb}_2\text{O}_5:\text{Mo}$ thin film and gelatin-based electrolyte. *Electrochimica Acta*, **53**, 1648–1654 (2007). DOI: [10.1016/j.electacta.2007.05.065](https://doi.org/10.1016/j.electacta.2007.05.065)

- [5] Machado G. O., Ferreira H. C. A., Pawlicka A.: Influence of plasticizer contents on the properties of HEC-based solid polymeric electrolytes. *Electrochimica Acta*, **50**, 3827–3831 (2005).
DOI: [10.1016/j.electacta.2005.02.041](https://doi.org/10.1016/j.electacta.2005.02.041)
- [6] Raphael E., Avellaneda C. O., Manzolli B., Pawlicka A.: Agar-based films for application as polymer electrolytes. *Electrochimica Acta*, **55**, 1455–1459 (2010).
DOI: [10.1016/j.electacta.2009.06.010](https://doi.org/10.1016/j.electacta.2009.06.010)
- [7] Florjanczyk Z., Debowski M., Chwojnowska E., Lokaj K., Ostrowska J.: Synthetic and natural polymers in modern polymeric materials. Part I. Polymers from renewable resources and polymer nanocomposites. *Polimery*, **54**, 691–705 (2009).
- [8] Aimé C., Coradin T.: Nanocomposites from biopolymer hydrogels: Blueprints for white biotechnology and green materials chemistry. *Journal of Polymer Science Part B: Polymer Physics*, **50**, 669–680 (2012).
DOI: [10.1002/polb.23061](https://doi.org/10.1002/polb.23061)
- [9] Legnani C., Vilani C., Calil V. L., Barud H. S., Quirino W. G., Achete C. A., Ribeiro S. J. L., Cremona M.: Bacterial cellulose membrane as flexible substrate for organic light emitting devices. *Thin Solid Films*, **517**, 1016–1020 (2008).
DOI: [10.1016/j.tsf.2008.06.011](https://doi.org/10.1016/j.tsf.2008.06.011)
- [10] Nogi M., Yano H.: Transparent nanocomposites based on cellulose produced by bacteria offer potential innovation in the electronics device industry. *Advanced Materials*, **20**, 1849–1852 (2008).
DOI: [10.1002/adma.200702559](https://doi.org/10.1002/adma.200702559)
- [11] Ohno H.: *Electrochemical aspects of ionic liquids*. Wiley, USA (2005).
- [12] Thayumanasundaram S., Piga M., Lavina S., Negro E., Jeyapandian M., Ghassemzadeh L., Müller K., Di Noto V.: Hybrid inorganic–organic proton conducting membranes based on Nafion, SiO₂ and triethylammonium trifluoromethanesulfonate ionic liquid. *Electrochimica Acta*, **55**, 1355–1365 (2010).
DOI: [10.1016/j.electacta.2009.05.079](https://doi.org/10.1016/j.electacta.2009.05.079)
- [13] Cheng H., Zhu C., Huang B., Lu M., Yang Y.: Synthesis and electrochemical characterization of PEO-based polymer electrolytes with room temperature ionic liquids. *Electrochimica Acta*, **52**, 5789–5794 (2007).
DOI: [10.1016/j.electacta.2007.02.062](https://doi.org/10.1016/j.electacta.2007.02.062)
- [14] Ohno H., Yoshizawa M., Ogihara W.: Development of new class of ion conductive polymers based on ionic liquids. *Electrochimica Acta*, **50**, 255–261 (2004).
DOI: [10.1016/j.electacta.2004.01.091](https://doi.org/10.1016/j.electacta.2004.01.091)
- [15] Kim G. T., Appetecchi G. B., Carewska M., Joost M., Balducci A., Winter M., Passerini S.: UV cross-linked, lithium-conducting ternary polymer electrolytes containing ionic liquids. *Journal of Power Sources*, **195**, 6130–6137 (2010).
DOI: [10.1016/j.jpowsour.2009.10.079](https://doi.org/10.1016/j.jpowsour.2009.10.079)
- [16] Kim J-K., Manuel J., Chauhan G. S., Ahn J-H., Ryu H-S.: Ionic liquid-based gel polymer electrolyte for LiMn_{0.4}Fe_{0.6}PO₄ cathode prepared by electrospinning technique. *Electrochimica Acta*, **55**, 1366–1372 (2010).
DOI: [10.1016/j.electacta.2009.05.043](https://doi.org/10.1016/j.electacta.2009.05.043)
- [17] Earle M. J., Esperança J. M. S. S., Gilea M. A., Lopes J. N. C., Rebelo L. P. N., Magee J. W., Seddon K. R., Widgren J. A.: The distillation and volatility of ionic liquids. *Nature*, **439**, 831–834 (2006).
DOI: [10.1038/nature04451](https://doi.org/10.1038/nature04451)
- [18] Smiglak M., Reichert W. M., Holbrey J. D., Wilkes J. S., Sun L., Thrasher J. S., Kirichenko K., Singh S., Katritzky A. R., Rogers R. D.: Combustible ionic liquids by design: Is laboratory safety another ionic liquid myth? *Chemical Communications*, **24**, 2554–2556 (2006).
DOI: [10.1039/B602086K](https://doi.org/10.1039/B602086K)
- [19] Baranyai K. J., Deacon G. B., MacFarlane D. R., Pringle J. M., Scott J. L.: Thermal degradation of ionic liquids at elevated temperatures. *Australian Journal of Chemistry*, **57**, 145–147 (2004).
DOI: [10.1071/CH03221](https://doi.org/10.1071/CH03221)
- [20] Takano R., Yoshikawa S., Ueda T., Hayashi K., Hirase S., Hara S.: Sulfation of polysaccharides with sulfuric acid mediated by dicyclohexylcarbodiimide. *Journal of Carbohydrate Chemistry*, **15**, 449–457 (1996).
DOI: [10.1080/07328309608005665](https://doi.org/10.1080/07328309608005665)
- [21] Xing D. Y., Peng N., Chung T-S.: Investigation of unique interactions between cellulose acetate and ionic liquid [EMIM]SCN, and their influences on hollow fiber ultrafiltration membranes. *Journal of Membrane Science*, **380**, 87–97 (2011).
DOI: [10.1016/j.memsci.2011.06.032](https://doi.org/10.1016/j.memsci.2011.06.032)
- [22] Kiefer J., Fries J., Leipertz A.: Experimental vibrational study of imidazolium-based ionic liquids: Raman and infrared spectra of 1-ethyl-3-methylimidazolium bis(trifluoromethylsulfonyl)imide and 1-ethyl-3-methylimidazolium ethylsulfate. *Applied Spectroscopy*, **61**, 1306–1311 (2007).
DOI: [10.1366/000370207783292000](https://doi.org/10.1366/000370207783292000)
- [23] Vitz J., Erdmenger T., Haensch C., Schubert U. S.: Extended dissolution studies of cellulose in imidazolium based ionic liquids. *Green Chemistry*, **11**, 417–424 (2009).
DOI: [10.1039/B818061J](https://doi.org/10.1039/B818061J)
- [24] Sadlej J., Jaworski A., Miaskiewicz K.: A theoretical study of the vibrational spectra of imidazole and its different forms. *Journal of Molecular Structure*, **274**, 247–257 (1992).
DOI: [10.1016/0022-2860\(92\)80161-A](https://doi.org/10.1016/0022-2860(92)80161-A)
- [25] Anglès M. N., Dufresne A.: Plasticized starch/tunicin whiskers nanocomposites. 1. Structural analysis. *Macromolecules*, **33**, 8344–8353 (2000).
DOI: [10.1021/ma0008701](https://doi.org/10.1021/ma0008701)

- [26] Prasad K., Mehta G., Meena R., Siddhanta A. K.: Hydrogel-forming agar-*graft*-PVP and κ -carrageenan-*graft*-PVP blends: Rapid synthesis and characterization. *Journal of Applied Polymer Science*, **102**, 3654–3663 (2006).
DOI: [10.1002/app.24145](https://doi.org/10.1002/app.24145)
- [27] Robitzer M., Tourrette A., Horga R., Valentin R., Boissière M., Devoisselle J. M., Di Renzo F., Quignard F.: Nitrogen sorption as a tool for the characterisation of polysaccharide aerogels. *Carbohydrate Polymers*, **85**, 44–53 (2011).
DOI: [10.1016/j.carbpol.2011.01.040](https://doi.org/10.1016/j.carbpol.2011.01.040)
- [28] Mitsuiki M., Mizuno A., Motoki M.: Determination of molecular weight of agars and effect of the molecular weight on the glass transition. *Journal of Agricultural and Food Chemistry*, **47**, 473–478 (1999).
DOI: [10.1021/jf980713p](https://doi.org/10.1021/jf980713p)
- [29] Li D-X., Liu B-L., Liu Y-S., Chen C-L.: Predict the glass transition temperature of glycerol–water binary cryoprotectant by molecular dynamic simulation. *Cryobiology*, **56**, 114–119 (2008).
DOI: [10.1016/j.cryobiol.2007.11.003](https://doi.org/10.1016/j.cryobiol.2007.11.003)
- [30] Freile-Pelegrín Y., Madera-Santana T., Robledo D., Veleza L., Quintana P., Azamar J. A.: Degradation of agar films in a humid tropical climate: Thermal, mechanical, morphological and structural changes. *Polymer Degradation and Stability*, **92**, 244–252 (2007).
DOI: [10.1016/j.polymdegradstab.2006.11.005](https://doi.org/10.1016/j.polymdegradstab.2006.11.005)
- [31] Vieira D. F., Avellaneda C. O., Pawlicka A.: A.C Impedance, X-Ray diffraction and DSC investigation on gelatin based-electrolyte with LiClO₄. *Molecular Crystals and Liquid Crystals*, **506**, 178 (2009).
DOI: [10.1080/15421400903162486](https://doi.org/10.1080/15421400903162486)
- [32] Raphael E., Avellaneda C. O., Aegerter M. A., Silva M. M., Pawlicka A.: Agar-based gel electrolyte for electrochromic device application. *Molecular Crystals and Liquid Crystals*, **554**, 264–272 (2012).
DOI: [10.1080/15421406.2012.634349](https://doi.org/10.1080/15421406.2012.634349)
- [33] Shaplov A. S., Lozinskaya E. I., Ponkratov D. O., Malyshkina I. A., Vidal F., Aubert P. H., Okatova O. V., Pavlov G. M., Komarova L. I., Wandrey C., Vygodskii Y. S.: Bis(trifluoromethylsulfonyl)amide based ‘polymeric ionic liquids’: Synthesis, purification and peculiarities of structure–properties relationships. *Electrochimica Acta*, **57**, 74–90 (2011).
DOI: [10.1016/j.electacta.2011.06.041](https://doi.org/10.1016/j.electacta.2011.06.041)
- [34] Marcondes R. F. M. S., D’Agostini P. S., Ferreira J., Giroto E. M., Pawlicka A., Dragunski D. C.: Amylopectin-rich starch plasticized with glycerol for polymer electrolyte application. *Solid State Ionics*, **181**, 586–591 (2010).
DOI: [10.1016/j.ssi.2010.03.016](https://doi.org/10.1016/j.ssi.2010.03.016)
- [35] Aurbach D., Daroux M., Faguy P., Yeager E.: The electrochemistry of noble metal electrodes in aprotic organic solvents containing lithium salts. *Journal of Electroanalytical Chemistry and Interfacial Electrochemistry*, **297**, 225–244 (1991).
DOI: [10.1016/0022-0728\(91\)85370-5](https://doi.org/10.1016/0022-0728(91)85370-5)
- [36] Nunes S. C., de Zea Bermudez V., Silva M. M., Smith M. J., Ostrovskii D., Sá Ferreira R. A., Carlos L. D., Rocha J., Gonçalves A., Fortunato E.: Sol–gel-derived potassium-based di-ureasils for ‘smart windows’. *Journal of Materials Chemistry*, **17**, 4239–4248 (2007).
DOI: [10.1039/B708905H](https://doi.org/10.1039/B708905H)
- [37] Lu J., Yan F., Texter J.: Advanced applications of ionic liquids in polymer science. *Progress in Polymer Science*, **34**, 431–448 (2009).
DOI: [10.1016/j.progpolymsci.2008.12.001](https://doi.org/10.1016/j.progpolymsci.2008.12.001)